

Myosin VI and its binding partner optineurin are involved in secretory vesicle fusion at the plasma membrane

Lisa M. Bond^{a,b}, Andrew A. Peden^a, John Kendrick-Jones^c, James R. Sellers^b, and Folma Buss^a

^aCambridge Institute for Medical Research, University of Cambridge, Cambridge CB2 0XY, United Kingdom;

^bLaboratory of Molecular Physiology, National Heart, Lung, and Blood Institute, National Institutes of Health,

Bethesda, MD 20892, USA; and ^cMRC Laboratory of Molecular Biology, Cambridge CB2 0QH, United Kingdom

ABSTRACT During constitutive secretion, proteins synthesized at the endoplasmic reticulum (ER) are transported to the Golgi complex for processing and then to the plasma membrane for incorporation or extracellular release. This study uses a unique live-cell constitutive secretion assay to establish roles for the molecular motor myosin VI and its binding partner optineurin in discrete stages of secretion. Small interfering RNA-based knockdown of myosin VI causes an ER-to-Golgi transport delay, suggesting an unexpected function for myosin VI in the early secretory pathway. Depletion of myosin VI or optineurin does not affect the number of vesicles leaving the *trans*-Golgi network (TGN), indicating that these proteins do not function in TGN vesicle formation. However, myosin VI and optineurin colocalize with secretory vesicles at the plasma membrane. Furthermore, live-cell total internal reflection fluorescence microscopy demonstrates that myosin VI or optineurin depletion reduces the total number of vesicle fusion events at the plasma membrane and increases both the proportion of incomplete fusion events and the number of docked vesicles in this region. These results suggest a novel role for myosin VI and optineurin in regulation of fusion pores formed between secretory vesicles and the plasma membrane during the final stages of secretion.

Monitoring Editor

Gero Steinberg

University of Exeter

Received: Jul 2, 2010

Revised: Oct 14, 2010

Accepted: Oct 21, 2010

INTRODUCTION

Constitutive exocytosis is a fundamental cellular process governing the transport of newly synthesized proteins to the cell surface for insertion into the plasma membrane or secretion into the extracellular environment. The secretory pathway involves a complex sequence of steps dependent on intracellular transport machinery. In the first stages of secretion, proteins synthesized by the ribosomes of the rough endoplasmic reticulum (ER) are transported in vesicles and larger tubular clusters from specific ER exit sites to the *cis* side

of the Golgi complex (Saraste and Svensson, 1991; Presley *et al.*, 1997). After the proteins are moved through the different compartments of the Golgi complex for posttranslational processing, they are sorted at the *trans* side of the Golgi complex into tubular or vesicular carriers and transported to the plasma membrane for exocytosis (Griffiths and Simons, 1986; Keller and Simons, 1997). The release of secreted proteins into the extracellular space during the final stages of secretion requires fusion of juxtaposed phospholipid bilayers of vesicular and plasma membranes to form an aqueous channel called a "fusion pore" that expands to permit full protein release (Jahn and Sudhof, 1999).

The intracellular transport system that coordinates the different stages of the secretory process is driven by carrier proteins called molecular motors. Transport by these motors can be divided into the short-range movements of myosin molecular motors along actin filament tracks and the comparatively faster and longer-ranged movements of kinesin and dynein motors along microtubule tracks. Within these three classes of motors lies the capacity for transport of secretory cargo in all directions within the cell: kinesin proteins primarily move cargo toward the plus ends of microtubules, dynein proteins transport cargo toward the minus ends of microtubules,

This article was published online ahead of print in MBoC in Press (<http://www.molbiolcell.org/cgi/doi/10.1091/mbc.E10-06-0553>) on December 9, 2010.

Address correspondence to: Folma Buss (fb1@mole.bio.cam.ac.uk).

Abbreviations used: ALS, amyotrophic lateral sclerosis; ER, endoplasmic reticulum; ERES, ER exit site; GalT, β -1,4-galactosyltransferase-1; GFP, green fluorescent protein; PBS, phosphate-buffered saline; POAG, primary open angle glaucoma; RFP, red fluorescent protein; SEAP, secreted form of alkaline phosphatase; siRNA, small interfering RNA; TGN, *trans*-Golgi network; TIRF, total internal reflection fluorescence.

© 2011 Bond *et al.* This article is distributed by The American Society for Cell Biology under license from the author(s). Two months after publication it is available to the public under an Attribution–Noncommercial–Share Alike 3.0 Unported Creative Commons License (<http://creativecommons.org/licenses/by-nc-sa/3.0>).

"ASCB®," "The American Society for Cell Biology®," and "Molecular Biology of the Cell®" are registered trademarks of The American Society of Cell Biology.

and specific myosin protein classes transport to either the plus or the minus ends of actin filaments. Cooperation between the three classes of molecular motors is thereby the driving force in the organization of trafficking in secretory transport processes. In addition to this well-defined role in cargo transport, molecular motor proteins have also been implicated in the organization of the secretory pathway through regulation of vesicle tethering and budding (Rudolf *et al.*, 2001; Egea *et al.*, 2006), cargo sorting and maintenance of morphology at the Golgi complex (Donaldson and Lippincott-Schwartz, 2000; Allan *et al.*, 2002; Sahlender *et al.*, 2005), and vesicle docking and fusion pore formation at the plasma membrane (Bhat and Thorn, 2009; Chung *et al.*, 2010).

One such motor protein suggested to function in the secretory pathway is myosin VI, which has the unique ability to transport cargo toward the minus ends of actin filaments (Wells *et al.*, 1999). Myosin VI localizes to vesicles in the perinuclear region at or around the Golgi complex (Buss *et al.*, 1998; Warner *et al.*, 2003) and to vesicles close to the plasma membrane (Sahlender *et al.*, 2005). Functional studies using fibroblasts isolated from the myosin VI knockout (Snell's waltzer) mouse or myosin VI small interfering RNA (siRNA) knockdown cells demonstrate a significant reduction in the constitutive exocytosis of a secreted form of alkaline phosphatase (SEAP) from cells lacking myosin VI (Warner *et al.*, 2003). Furthermore, myosin VI is required for the delivery of newly synthesized transmembrane proteins to the basolateral plasma membrane domain in polarized epithelial cells. In these cells, depletion of functional myosin VI by overexpression of the dominant negative tail domain results in a missorting of basolateral cargo such as vesicular stomatitis virus G-protein (VSV-G) to the apical plasma membrane (Au *et al.*, 2007; Chibalina *et al.*, 2008). These data clearly establish a role for myosin VI in secretion, but they provide no insight as to the specific involvement of myosin VI throughout the stages of the secretory pathway.

The role of myosin VI in the secretory pathway is closely linked to its interacting protein optineurin. Optineurin is a 67-kDa dimeric protein that colocalizes with myosin VI in the perinuclear region and on vesicles beneath the plasma membrane (Sahlender *et al.*, 2005). siRNA-mediated knockdown of optineurin decreases secretion of SEAP and VSV-G in a similar manner to myosin VI depletion (Sahlender *et al.*, 2005; Au *et al.*, 2007; Chibalina *et al.*, 2008). Optineurin not only binds to myosin VI but has also been shown to interact with the GTPase Rab8 and with huntingtin, which are important regulators of vesicle transport (Huber *et al.*, 1993b; Hattula and Peranen, 2000; Caviston and Holzbaur, 2009). Recent implications that defects in optineurin cause primary open angle glaucoma (POAG) (Rezaie *et al.*, 2002) and play a role in the pathogenesis of amyotrophic lateral sclerosis (ALS) (Maruyama *et al.*, 2010) stress the importance of investigating its primary intracellular functions.

Although previous work has established a role for myosin VI and optineurin in constitutive secretion of a variety of transmembrane proteins and soluble luminal cargo in both polarized and unpolarized cells, no available studies address the specific roles of these proteins in the secretory pathway. Therefore, in this study, we investigate the exact roles of myosin VI and optineurin at each stage of constitutive secretion using live-cell fluorescence microscopy on a HeLa cell line stably expressing a green fluorescent protein (GFP)-tagged reporter construct (Gordon *et al.*, 2010). We are able to demonstrate an unexpected role for myosin VI in the ER-to-Golgi transport stage of secretion, because depletion of myosin VI leads to a kinetic delay in cargo transport between the ER and Golgi complex. Interestingly, our results further suggest that myosin VI and optineurin are not required for transport carrier formation at the *trans*-Golgi network (TGN). However, we demonstrate that myosin VI and

optineurin colocalize with secretory vesicles at the plasma membrane. Furthermore, loss of myosin VI or optineurin dramatically reduces the number of cargo vesicles fusing with the plasma membrane and increases both the number of incomplete fusion events and the number of docked vesicles at the plasma membrane. Taken together, these results suggest a role for myosin VI and optineurin in the mechanical regulation of the fusion pore that opens to permit protein release in the final stages of the secretory pathway.

RESULTS

To examine the specific roles of myosin VI and optineurin in the secretory pathway, we used a HeLa cell line stably expressing a GFP-tagged reporter construct (Gordon *et al.*, 2010). This reporter construct contains multiple aggregation domains and remains arrested in an aggregated form in the ER after synthesis. Binding of the small ligand AP21998 (Ariad Pharmaceuticals, Cambridge, MA) to the aggregation domains yields soluble protein, allowing a synchronous pulse of GFP-tagged reporter construct to be transported from the ER to the Golgi complex and then to the plasma membrane for release from the cell. This regulated secretion system permits visualization of the main stages of constitutive secretion via live-cell time-lapse fluorescence microscopy.

Knockdown of myosin VI causes a kinetic delay in ER-to-Golgi transport

To establish the exact role(s) of myosin VI and optineurin in the secretory pathway, we first investigated the involvement of these proteins in the earliest transport-driven stage of secretion: the delivery of synthesized proteins from the ER to the Golgi complex. For this study, cells in our assay system were imaged using live-cell spinning disc microscopy for a 30-min period immediately following AP21998 treatment to monitor delivery of the GFP-tagged reporter molecule from the ER into the Golgi region. The position of the Golgi complex was visualized by expressing a red fluorescent protein (RFP)-tagged β -1,4-galactosyltransferase-I (GalT) construct. Still images of a video showing movement of the reporter molecule from the ER into the Golgi complex in a mock treated cell are shown in the top of Figure 1A. The time-lapse images in the bottom of Figure 1A display the delay in accumulation of cargo in the Golgi region observed in a cell in which myosin VI has been depleted with a 5-d, double-hit siRNA knockdown protocol. At each time point, significantly less GFP-tagged reporter molecule is present in the Golgi complex in this myosin VI knockdown cell, as compared with the mock cell in the top panel.

To quantify the rate of reporter construct transfer from the ER to the Golgi complex, Volocity analysis software was used to track the accumulation of fluorescent reporter construct intensity in the region defined as the Golgi complex by the GalT-RFP marker protein. The fluorescent intensity present in the Golgi region at each time point was converted to a percentage of the total fluorescent intensity in the cell present before addition of AP21998 and plotted versus time to the point of maximum Golgi fluorescence. The slope of this plot represents the rate of reporter construct transport from the ER to the Golgi complex. This method was used to calculate the rate of reporter construct transfer between ER and Golgi in cells in which myosin VI or optineurin had been depleted by siRNA transfection (Figure 1C). Optineurin SMARTpool knockdown cells show no significant difference in average ER-to-Golgi transport rate when compared with mock cells (Figure 1B). However, knockdown of myosin VI with a SMARTpool collection of four siRNA primers or with distinct, individual siRNA primers consistently results in a reduction in ER-to-Golgi transport rate, as compared with mock cells (38% overall average rate reduction) (Figure 1B).

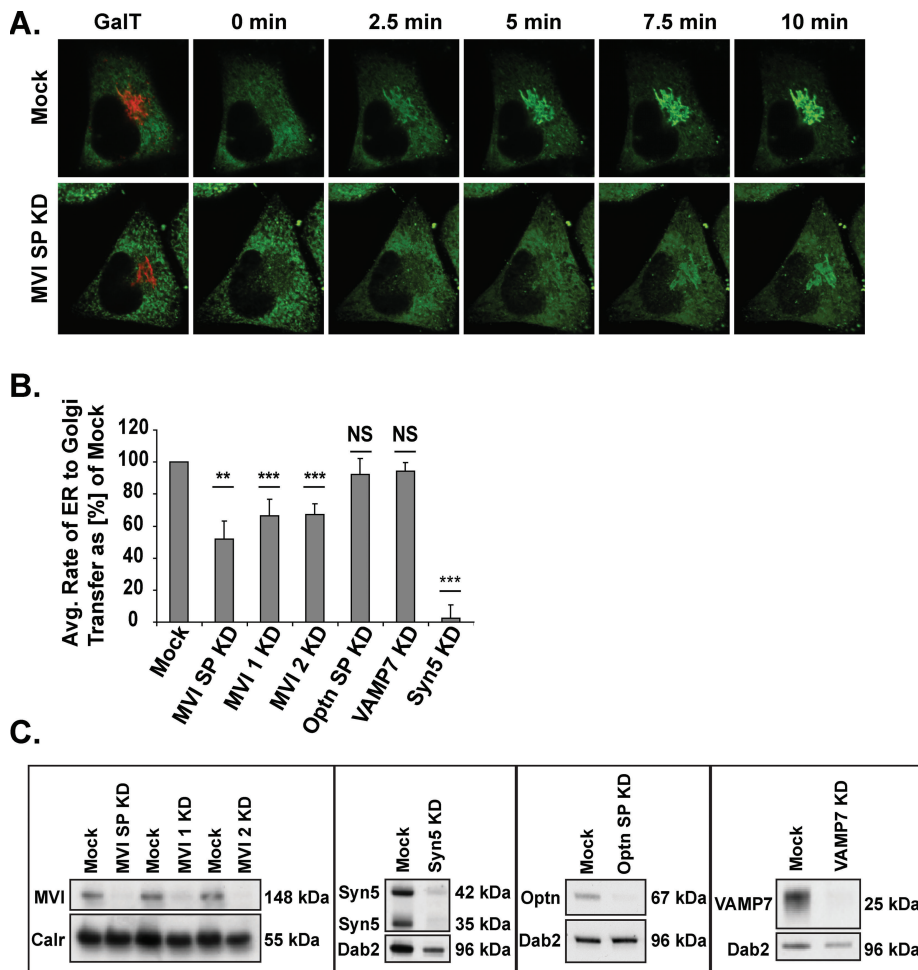


FIGURE 1: Rate of reporter molecule transport from the ER to the Golgi complex. (A) Time-lapse images illustrating the accumulation of reporter molecule fluorescence in the Golgi region (as labeled with GalT-RFP) over the first 10 min after AP21998 addition to a mock cell (top row) or to a myosin VI knockdown cell (bottom row). (B) Rate of ER-to-Golgi reporter molecule transfer in sets of two to eight knockdown cells as a percentage of mock. Knockdown of myosin VI with SMARTpool primers (SP), individual primer 1, or individual primer 2 results in 48, 34, or 33% decreases in ER-to-Golgi transport rate, respectively (unpaired t test; $n = 5, 4, 5$ experimental sets; $p = 0.005, p = 3 \times 10^{-8}, p = 3 \times 10^{-10}$). Knockdown of optineurin or VAMP7 has no significant effect on the rate of ER to Golgi transport (unpaired t test; $n = 4, 6$ experimental sets; $p = 0.3, p = 0.6$), while a knockdown of syntaxin5 results in a 97% decrease in this rate (unpaired t test; $n = 6$ experimental sets; $p = 8 \times 10^{-8}$). Error bars represent standard error of the mean (SEM). * $p \leq 0.05$, ** $p \leq 0.01$, *** $p \leq 0.001$. (C) Western blot analysis of siRNA knockdown of optineurin, myosin VI, VAMP7, and syntaxin5.

As a control, the same rate analysis study was conducted in cells depleted of two distinct members of the SNARE family, a group of proteins that mediate vesicle docking and fusion (Figure 1C). Knockdown of the vesicle-associated membrane protein 7 (VAMP7), a post-Golgi SNARE, has no significant effect on ER-to-Golgi transport (Figure 1B), which indicates that the delay in transport seen after a knockdown of myosin VI is not simply a result of our siRNA knockdown protocol. Knockdown of the ER-to-Golgi SNARE syntaxin5, however, completely inhibits ER-to-Golgi transport (Figure 1B), suggesting that a knockdown of myosin VI results in a kinetic delay rather than a complete block in ER-to-Golgi transport. Overall, our results suggest an unexpected role for myosin VI in the transport of cargo between the ER and the Golgi complex during the early stages of the secretory pathway.

Myosin VI and optineurin colocalize with secretory vesicles at the plasma membrane

We examined the involvement of myosin VI and optineurin in the later stages of the secretory pathway using total internal reflection fluorescence (TIRF) microscopy, a technique that permits the selective illumination of the 100–200-nm region nearest the plasma membrane at the base of the cell. Because the localization of optineurin and myosin VI relative to vesicles in this proximity of the plasma membrane has not previously been demonstrated, we used TIRF microscopy with fixed, immunofluorescence-labeled cells to examine the distribution of myosin VI and optineurin with respect to secretory vesicles in the TIRF field.

For these immunofluorescence studies, HeLa cells stably expressing the GFP-tagged reporter construct were treated with AP21998 and fixed 35 min after treatment. To examine the localization of

The number of secretory vesicles traveling out of the Golgi complex is not changed, however, in myosin VI or optineurin knockdown cells

To determine whether the delay in ER-to-Golgi protein transfer after depletion of myosin VI is propagated to the post-Golgi stages of the secretory pathway and whether myosin VI and optineurin are required for vesicle formation at the TGN, we next assayed the number of vesicles leaving the Golgi complex in mock versus myosin VI or optineurin knockdown cells. For this analysis, we took 1-min, confocal spinning disc videos of sections through the middle of the cell at specific intervals between 25 and 60 min after AP21998 addition. Vesicle tracking software designed at the National Institutes of Health and Emory University was used to quantify the number of individual vesicles present in $6 \mu\text{m} \times 6 \mu\text{m}$ regions between the *trans*-Golgi and plasma membrane over the course of these videos (Figure 2). Comparison of mock and siRNA SMARTpool knockdown cells reveals that the depletion of myosin VI or optineurin results in no significant change in the number of vesicles traveling through these regions. This indicates that the reduced transport rate between the ER and Golgi complex in myosin VI knockdown cells is not a rate-limiting step in the overall secretory process and does not reduce the number of cargo vesicles leaving the *trans* side of the Golgi complex. This enables us to study the involvement of myosin VI and optineurin in the post-Golgi stages of the pathway independently of defects observed in the early steps of the secretory pathway. Furthermore, these results suggest that myosin VI and optineurin are unlikely to play a major role in vesicle formation at the TGN as previously speculated (Buss and Kendrick-Jones, 2008).

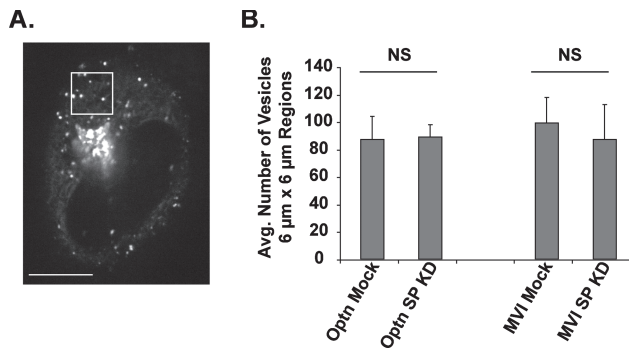


FIGURE 2: Number of vesicles traveling between the Golgi and plasma membrane. (A) Illustration of vesicle numbering method. The image displays a cell in which one $6\ \mu\text{m} \times 6\ \mu\text{m}$ region between the Golgi complex and the plasma membrane has been selected. For analysis, the total number of vesicles present in regions of this size and location were quantified over the course of 1-min videos using vesicle tracking software. (B) Average number of vesicles in $6\ \mu\text{m} \times 6\ \mu\text{m}$ regions between the Golgi and plasma membrane in mock, optineurin, or myosin VI knockdown cells. Data represent averages of the total number of vesicles in $6\ \mu\text{m} \times 6\ \mu\text{m}$ regions placed in sets of five cells imaged at specific intervals between 25 and 60 min after the addition of AP21998. There is no significant difference in the number of vesicles present in these regions after a knockdown of optineurin (unpaired *t* test; *n* = 3 experimental sets; *p* = 0.9) or a knockdown of myosin VI (unpaired *t* test; *n* = 3 experimental sets; *p* = 0.7). Error bars represent SEM. **p* ≤ 0.05, ***p* ≤ 0.01, ****p* ≤ 0.001.

myosin VI with respect to GFP-tagged secretory cargo, fixed cells transfected with an mCherry-myosin VI construct were labeled with a monoclonal antibody to GFP [cargo, Figure 3A(a)] and a polyclonal antibody for mCherry [myosin VI construct, Figure 3A(b)]. The high level of colocalization between myosin VI and cargo-containing secretory vesicles at the plasma membrane [Figure 3A(c)] directly suggests a role for myosin VI in the later stages of the secretory pathway. Depletion of optineurin by siRNA knockdown does not affect this colocalization of myosin VI and secretory vesicles at the plasma membrane (unpublished data). To examine the localization of optineurin with respect to secretory cargo, fixed cells were labeled with a monoclonal antibody to GFP [cargo, Figure 3B(a)] and a polyclonal antibody to optineurin [optineurin, Figure 3B(b)]. This low-level colocalization of optineurin with specific secretory vesicles [Figure 3B(c)] suggests a potential role for optineurin in the final stages of secretion.

The number of secretory vesicle fusion events at the plasma membrane is decreased by a knockdown of myosin VI or optineurin

To examine the function of the myosin VI and optineurin associated with late-stage secretory cargo, we conducted TIRF microscopy experiments with live cells. The use of TIRF to selectively illuminate the 100–200-nm region nearest the plasma membrane at the base of a live cell increases the signal-to-noise ratio to such an extent that it is possible to visualize the fusion of individual, cargo-filled secretory vesicles with the plasma membrane (Zenisek *et al.*, 2000). Such fusion events represent the formation of a small, aqueous channel or “fusion pore” between the membrane of a vesicle docked at the plasma membrane and the plasma membrane itself (Jahn and Sudhof, 1999). This fusion pore dilates to permit the release of secretory proteins from the vesicle into the extracellular environment (Sorensen, 2009). In our study, the rapid, extracellular release of the fluorescently tagged reporter construct during an individual vesicle

fusion event can be observed as a sudden, punctate flash of light in the TIRF field. It is thus possible to quantify the number of individual fusion events in a given cell by counting the number of punctate flashes of light observed at the cell base using TIRF microscopy.

To determine the effects of an absence of myosin VI or optineurin on vesicle fusion at the plasma membrane, we quantified the total number of fusion events in sets of mock or siRNA knockdown cells monitored at specific, 5-min intervals between 25 and 60 min after AP21998 treatment. Still images of videos taken in the TIRF field of mock, optineurin, myosin VI, or Rab8 knockdown cells are shown in Figure 4A. Pink squares mark the sites of fusion events during a 20-s time-lapse movie. When compared with mock cells, knockdown of optineurin with a SMARTpool collection of four siRNA primers results in a 50% average decrease in the total number of fusion events, whereas knockdown of myosin VI with SMARTpool primers results in a 38% average decrease (Figure 4B). Supplemental Movies 1–3 provide a visual demonstration of this decrease in fusion events after a knockdown of myosin VI or optineurin.

To control for possible off-target effects, we performed the same study with individual siRNA primers for both optineurin and myosin VI. Knockdowns with two individual primers for optineurin result in very consistent 47% decreases in the total number of fusion events (Figure 4B). Similarly, knockdowns with two individual primers for myosin VI result in consistent 34 and 37% decreases in the total number of fusion events (Figure 4B). These data indicate that the decrease in fusion events observed after a SMARTpool knockdown of optineurin or myosin VI is not simply an off-target effect of the siRNA primers.

We also measured fusion events at the plasma membrane in Rab8 knockdown cells (Figure 4C) to assess whether this protein, an optineurin-interacting protein and GTPase involved in post-Golgi membrane trafficking, is required for secretory vesicle fusion at the plasma membrane. The results summarized in Figure 4B show that loss of Rab8 expression has no significant effect on the average number of fusion events and so indicate that this Rab protein is not required in the final stages of the secretory pathway. Supplemental Movies 1 and 4 provide a visual demonstration of this similar level of fusion events in mock versus Rab8 knockdown cells.

An increased number of vesicles are docked in the 100–200-nm TIRF field in cells depleted of myosin VI or optineurin

To test whether the decrease in fusion events after a knockdown of optineurin or myosin VI results in an increase in the number of docked vesicles present at the plasma membrane, we quantified the total area in the TIRF field occupied by docked vesicles in sets of 10 mock and knockdown cells imaged at specific intervals between 25 and 60 min after AP21998 addition. The top panel in Figure 5A presents representative images of the TIRF field of mock and knockdown cells. Confocal spinning disc images of the plasma membrane at the base of sample mock and knockdown cells are presented in the bottom panel as a reference point for the observation of differences in vesicle content with higher *x-y* resolution.

Knockdown of optineurin results in an 83% increase in the area of the TIRF field occupied by docked vesicles and a knockdown of myosin VI similarly results in a 70% increase in this area, as compared with mock cells (Figure 5B). In Rab8 knockdown cells, no significant increase in the area of the TIRF field occupied by docked vesicles is observed (Figure 5B). This increase in the relative proportion of docked vesicles present within 100–200 nm of the plasma membrane after a knockdown of myosin VI or optineurin suggests a

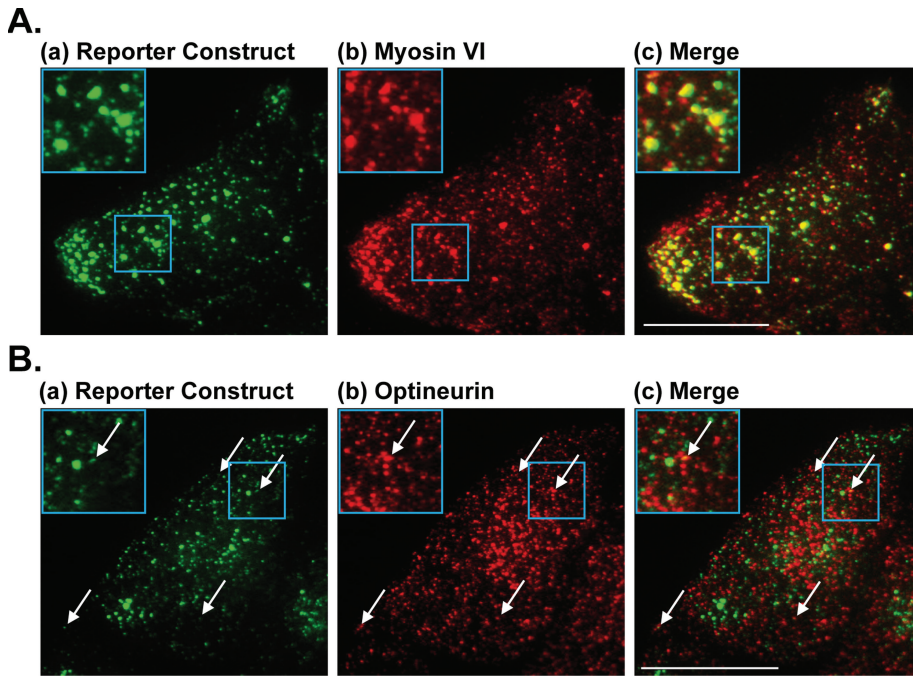


FIGURE 3: Colocalization of myosin VI and optineurin with secretory vesicles at the plasma membrane. (A) Sample images of the TIRF field at the base of a HeLa cell (a) stably expressing the GFP-tagged reporter construct and (b) transfected with an mCherry-tagged myosin VI construct. Cells were fixed 35 min after AP21998 addition and labeled by immunofluorescence with a polyclonal antibody for mCherry and a monoclonal antibody to GFP. (c) A high level of colocalization is visible between myosin VI and secretory vesicles in the TIRF field containing the reporter construct. Blue boxes highlight the region expanded for closer viewing in the top left of each panel. Bar, 10 μm . (B) Sample images of the TIRF field at the base of a fixed HeLa cell (a) stably expressing the GFP-tagged reporter construct and (b) labeled for endogenous optineurin. Cells were fixed 35 min after AP21998 addition and labeled by immunofluorescence with a polyclonal antibody to optineurin and a monoclonal antibody to GFP. (c) A low level of colocalization is visible between optineurin and the secretory vesicles in the TIRF field. White arrows point out specific examples of colocalization and the blue boxes highlight the example expanded in the top left of each panel. Bar, 10 μm .

role for myosin VI and optineurin in the final, vesicle fusion stages of the secretory pathway.

The proportion of incomplete secretory vesicle fusion events at the plasma membrane is increased in myosin VI or optineurin knockdown cells

In our TIRF time-lapse movies, we observe two distinct types of exocytic fusion events during the constitutive secretion of the reporter molecule (Figure 6). The primary type (96% of fusion events in mock cells) can be visualized as a transient flash of spreading and then disappearing fluorescent light (Figure 6B, images) and fits the profile of the “full fusion events” described in previous studies of vesicle fusion (Jahn and Sudhof, 1999; Steyer and Almers, 2001; Jackson and Chapman, 2006; Sorensen, 2009). These full fusion events occur in a series of stages: the secretory vesicle docks at the plasma membrane, the vesicle is primed as fusion machinery gathers, a small fusion pore is formed as the vesicle membrane and plasma membrane fuse to create an aqueous channel, and finally the fusion pore expands to permit rapid release of vesicle contents from the cell by diffusion (Jackson and Chapman, 2006). Quantitative modeling of the average fluorescent intensity in the area immediately surrounding a full fusion event reveals a characteristic peak shape (Figure 6B, graph) in which the upward portion of the graph represents the movement of the vesicle toward the plasma membrane, the

peak of the graph represents the formation of a fusion pore with the vesicular membrane (“fusion”), and the downward slope of the graph represents the release of the fluorescent reporter molecule through the expanded fusion pore. In such a full fusion event, the average fluorescent intensity in the seconds (–5 to –1) immediately prior to the fusion peak is characteristically higher than the average fluorescent intensity in the seconds (+1 to +5) immediately following the fusion peak, reflecting the fact that the fluorescent reporter construct is fully released from the fused vesicle.

Four percent of the vesicles in mock cells exhibit a second type of fusion pattern, in which a docked vesicle flashes briefly and then remains present and filled with fluorescent cargo beneath the plasma membrane (Figure 6B, images). The behavior of these vesicles fits the profile of the “incomplete fusion events” previously observed by patch amperometry or capacitance recording (Spruce *et al.*, 1990; Zhou *et al.*, 1996; Albillos *et al.*, 1997). In these incomplete fusion events, vesicles dock, prime, form transient fusion pores with the plasma membrane, and then close these pores rather than expanding them for full cargo release (Sorensen, 2009). Quantitative modeling of the average fluorescent intensity in the area immediately surrounding an incomplete fusion event reveals a characteristic peak shape (Figure 6B, graph) in which the average fluorescent intensity in the seconds (–5 to –1) immediately prior to the fusion peak is lower than the average fluorescent intensity in the seconds (+1 to +5) immediately following the fusion peak, reflecting an incomplete release of fluorescent cargo. The color-coded boxes in Supplemental Movies 1–4 highlight the appearance of full versus incomplete fusion events as observed by live-cell TIRF microscopy.

To further characterize the exact role of myosin VI and optineurin in the later secretory pathway, we assessed whether the decrease in full fusion events at the plasma membrane after a knockdown of myosin VI or optineurin is accompanied by a corresponding increase in incomplete secretory vesicle fusion events. Still images of videos taken in the TIRF field of mock, optineurin, myosin VI, and Rab8 knockdown cells are shown in Figure 6A. Blue squares mark the sites of full fusion events and red squares mark the sites of incomplete fusion events during a 20-s time-lapse movie. For our study, we quantified the proportion of total vesicle fusion events that did not proceed to a full release of the fluorescent reporter molecule (“proportion of incomplete fusion events”) in sets of cells monitored at specific, 5-min intervals between 25 and 60 min after AP21998 treatment (Figure 6C). Strikingly, cells in which optineurin has been knocked down with a SMARTpool primer collection or with individual primers have an eight- to ninefold higher proportion of incomplete fusion events than mock cells. Cells in which myosin VI has been knocked down with SMARTpool or individual primers also display a 1.6- to 1.7-fold increase in the proportion of incomplete fusion events when compared with mock cells. Rab8 knockdown cells,

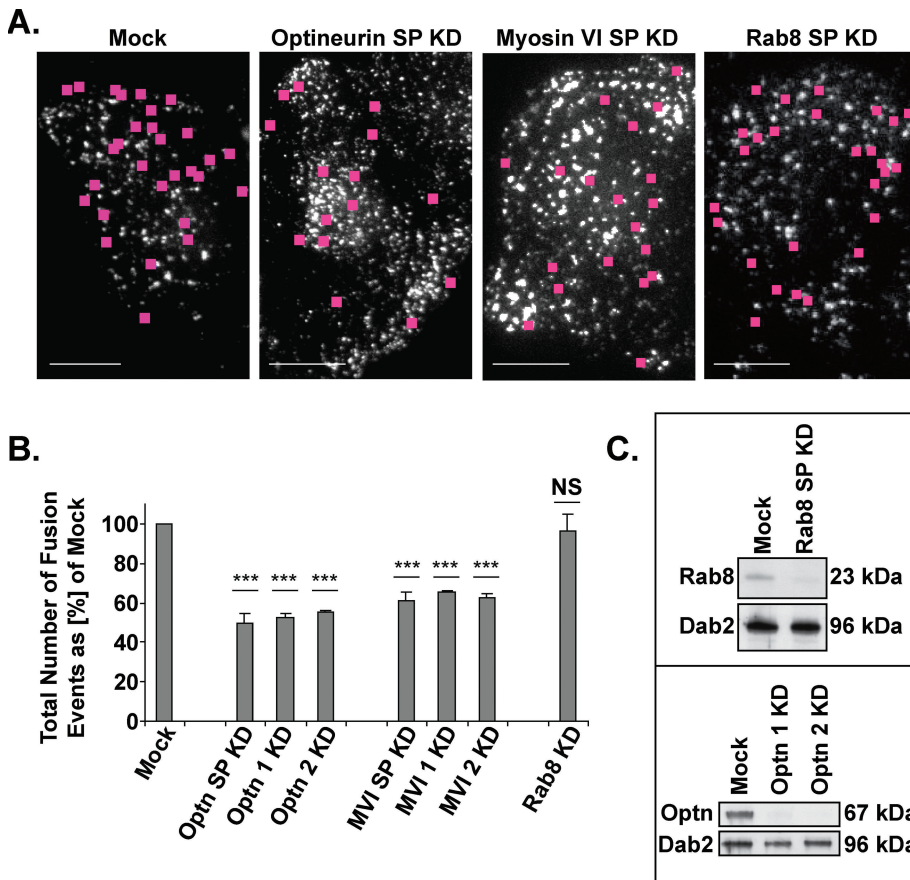


FIGURE 4: Total number of vesicle fusion events at the plasma membrane. (A) Sample images of the TIRF field of mock and knockdown cells with pink squares marking the sites of fusion events over the course of a 20-s movie. Bars, 10 μ m. (B) Average total number of vesicle fusion events observed by TIRF microscopy at the base of sets of cells monitored at specific, 5-min intervals between 25 and 60 min after AP21998 addition. Knockdown of optineurin with SMARTpool primers (SP), individual primer 1, or individual primer 2 results in a 50, 47, or 47% decrease in the total number of vesicle fusion events, respectively (unpaired t test; $n = 4$ sets of 10 cells each [SP] or 4 sets of five cells each [individual primers]; $p = 9 \times 10^{-6}$, $p = 2 \times 10^{-5}$, $p = 1 \times 10^{-5}$). Knockdown of myosin VI with SMARTpool primers (SP), individual primer 1, or individual primer 2 results in a 38, 34, or 37% decrease in the total number of vesicle fusion events, respectively (unpaired t test; $n = 5$ sets of 10 cells each [SP] or 4 sets of five cells each [individual primers]; $p = 9 \times 10^{-5}$, $p = 7 \times 10^{-5}$, $p = 7 \times 10^{-5}$). Knockdown of Rab 8 has no significant effect on the total number of vesicle fusion events (unpaired t test; $n = 3$ sets of 10 cells each; $p = 0.9$). Error bars represent SEM. * $p \leq 0.05$, ** $p \leq 0.01$, *** $p \leq 0.001$. (C) Western blot analysis of siRNA knockdown of Rab8 with SMARTpool primers and of optineurin with individual primers 1 and 2.

however, show no significant difference from mock cells in the proportion of vesicle fusion events that do not proceed to completion. Supplemental Movies 1–4 provide a visual demonstration of the increase in incomplete fusion events after a knockdown of myosin VI or optineurin and the unchanged proportion of incomplete fusion events after a knockdown of Rab8. The decrease in full fusion events and increase in incomplete fusion events observed after depletion of optineurin or myosin VI directly suggests a role for these proteins in the pore expansion stage necessary for full cargo release by secretory vesicles at the plasma membrane.

DISCUSSION

Although a requirement for myosin VI and its interacting protein optineurin in protein secretion has been established using a variety of assays in different cell types, the exact molecular role of these proteins in the exocytic pathway is unknown. Using a unique live-cell secretion assay that allows visualization of the synchronized traffick-

ing of a GFP-tagged reporter molecule from the ER through the Golgi complex to the plasma membrane, we are able to establish roles for myosin VI and optineurin at discrete stages of secretion. Specifically, our results indicate an unexpected function for myosin VI in ER to Golgi transport and a role for both myosin VI and optineurin in secretory vesicle fusion at the plasma membrane.

Role for myosin VI in ER-to-Golgi transport

The kinetic delay in ER-to-Golgi transport visible after a knockdown of myosin VI suggests a role for this protein in the early stages of secretion. It is possible that myosin VI plays a novel mechanistic role in this stage of the secretory pathway. Though microtubule-based transport is the classic mode of transport of COPII-coated vesicles from ER exit sites (ERESs) to the central Golgi complex (Palmer *et al.*, 2005), a complementary role for the actin cytoskeleton in COPII vesicle transport has been suggested (Disanza and Scita, 2008). Myosin VI proteins moving along such ERES-associated actin filaments could play a role in mediating COPII exit from the ER, tethering COPII vesicles near ERESs, or transporting these vesicles in shorter-range movements along actin filaments before their longer-range transport along microtubules. Alternatively, the kinetic delay that we note in ER-to-Golgi transport may be an indirect result of modifications in the actin cytoskeleton upon depletion of myosin VI. Myosin VI has been implicated in the organization of the actin cytoskeleton (Noguchi *et al.*, 2006), and the bidirectional transport of cargo between ERESs and the Golgi complex likely relies partially on actin-based transport (Lee *et al.*, 2004). Whether direct or indirect, our

results suggest a novel influence of myosin VI on ER-to-Golgi secretion.

Golgi-to-plasma membrane transport

Interestingly, the number of vesicles budding and traveling away from the TGN is not changed by a myosin VI knockdown, despite the observed kinetic delay in ER-to-Golgi transport upon depletion of myosin VI. This finding suggests that the moderate reduction in transport rate between the ER and Golgi complex after myosin VI depletion is not a rate-limiting factor in the overall secretory pathway and so does not affect the transport levels between the Golgi and the plasma membrane.

Myosin VI and optineurin are both associated with vesicular structures in the perinuclear region around the Golgi complex and have therefore been suggested to play a role in secretory vesicle formation or cargo sorting at the TGN (Buss and Kendrick-Jones, 2008). Our results, however, do not support a critical role for myosin

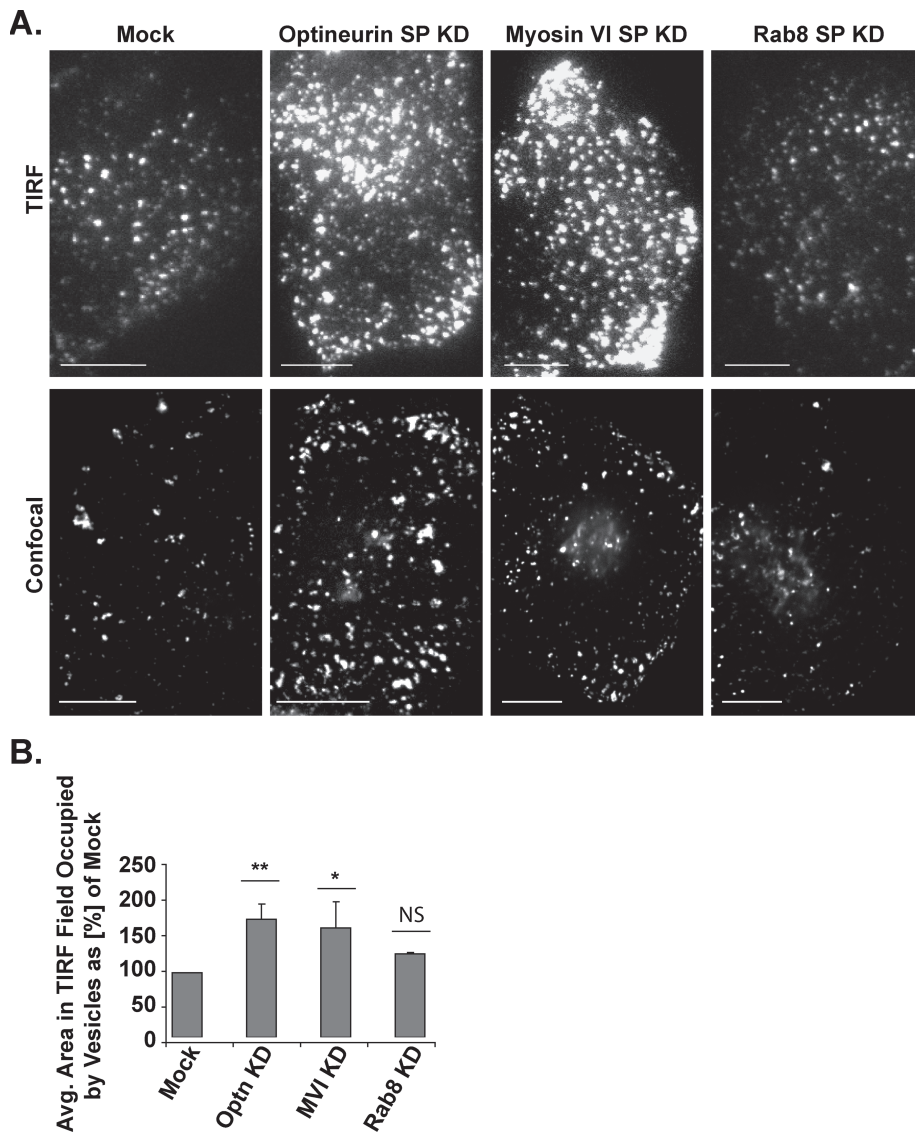


FIGURE 5: Relative area of the TIRF field occupied by vesicles. (A) Top, sample images of vesicles in the TIRF field at the base of mock, optineurin knockdown, myosin VI knockdown, and Rab8 knockdown cells. Bottom, confocal images at the base of mock and knockdown cells as a reference for vesicle content at a higher x-y resolution. Bar, 10 μ m. (B) Relative average area of the TIRF field occupied by docked vesicles. Volocity analysis software was used to calculate the total area in the TIRF field occupied by fluorescent vesicles in single plane images taken at specific intervals between 25 and 60 min after AP21998 addition to mock and knockdown cells. Knockdown of optineurin results in an 83% increase in the area occupied by vesicles as compared with mock cells (unpaired t test; $n = 3$ sets of 10 cells; $p = 0.008$) and knockdown of myosin VI similarly results in a 70% increase in the area occupied by vesicles (unpaired t test; $n = 3$ sets of ten cells; $p = 0.04$). A knockdown of Rab8, however, has no significant effect on the area in the TIRF field occupied by vesicles (unpaired t test; $n = 3$ sets of 10 cells; $p = 0.2$). Bar, SEM. * $p \leq 0.05$, ** $p \leq 0.01$, *** $p \leq 0.001$.

VI or optineurin in the basic mechanism of vesicle formation at the TGN, because we do not observe any change in the number of vesicles traveling from the TGN to the plasma membrane in myosin VI or optineurin knockdown cells. The perinuclear localization of myosin VI and optineurin may therefore be linked to a function in cargo sorting rather than vesicle formation at the TGN. This hypothesis is supported by previous findings that myosin VI and optineurin function with Rab8 in cargo sorting to the basolateral domain in polarized epithelial cells and to the dendritic surface in neuronal cells (Huber *et al.*, 1993a; Au *et al.*, 2007). Because unpolari-

zed HeLa cells do not sort cargo to specific plasma membrane domains, such cargo sorting defects could not be identified for the reporter molecule used in this study.

Role for optineurin and myosin VI in fusion pore expansion at the plasma membrane

Using TIRF microscopy, we have demonstrated colocalization of myosin VI and optineurin with secretory vesicles at the plasma membrane and established that the absence of optineurin or myosin VI has a dramatic effect on the final stages of the secretory pathway. In myosin VI or optineurin knockdown cells, we observe a 35–50% decrease in the number of secretory vesicles fusing with the plasma membrane for protein release into the extracellular space. This reduction in the total number of fusion events is very similar to the previously reported ~50% decrease in constitutive secretion of reporter molecules such as VSV-G or SEAP in optineurin or myosin VI siRNA knockdown cells or in fibroblasts isolated from the myosin VI knockout mouse (Sahlender *et al.*, 2005; Chibalina *et al.*, 2008).

The fact that our observed reduction in the total number of fusion events is accompanied by an increased number of docked vesicles beneath the plasma membrane focuses the secretory defect arising from a knockdown of myosin VI or optineurin to the final stages of the secretory pathway (docking, priming, or vesicle fusion). Our detailed examination of the fusion defect demonstrates that knockdown of optineurin or myosin VI results specifically in an increase in the proportion of incomplete fusion events. This result would appear to link the defect to a change in the behavior of the fusion pore formed between the vesicle membrane and plasma membrane during the final stages of secretion. Because the opening and closing of exocytic fusion pores is believed to be a dynamic and reversible process (Jackson and Chapman, 2006), our observed increase in instances of incomplete cargo release from fused vesicles suggests that a knockdown of optineurin or myosin VI either hinders the outward expansion of fusion pores during exocytosis or increases the frequency of reversible closure of these pores.

Such involvement of an actin-based molecular motor in fusion pore mechanics is not without precedent. Myosin II has been shown to maintain an open fusion pore in secretory epithelial cells and a mutant form of myosin II hinders fusion pore expansion during secretion in chromaffin cells (Neco *et al.*, 2008; Bhat and Thorn, 2009). Related studies tie the role of myosin II in fusion pore mechanics closely to its interaction with the actin cytoskeleton (Becker and Hart, 1999; Doreian *et al.*, 2008; Berberian *et al.*, 2009), which has

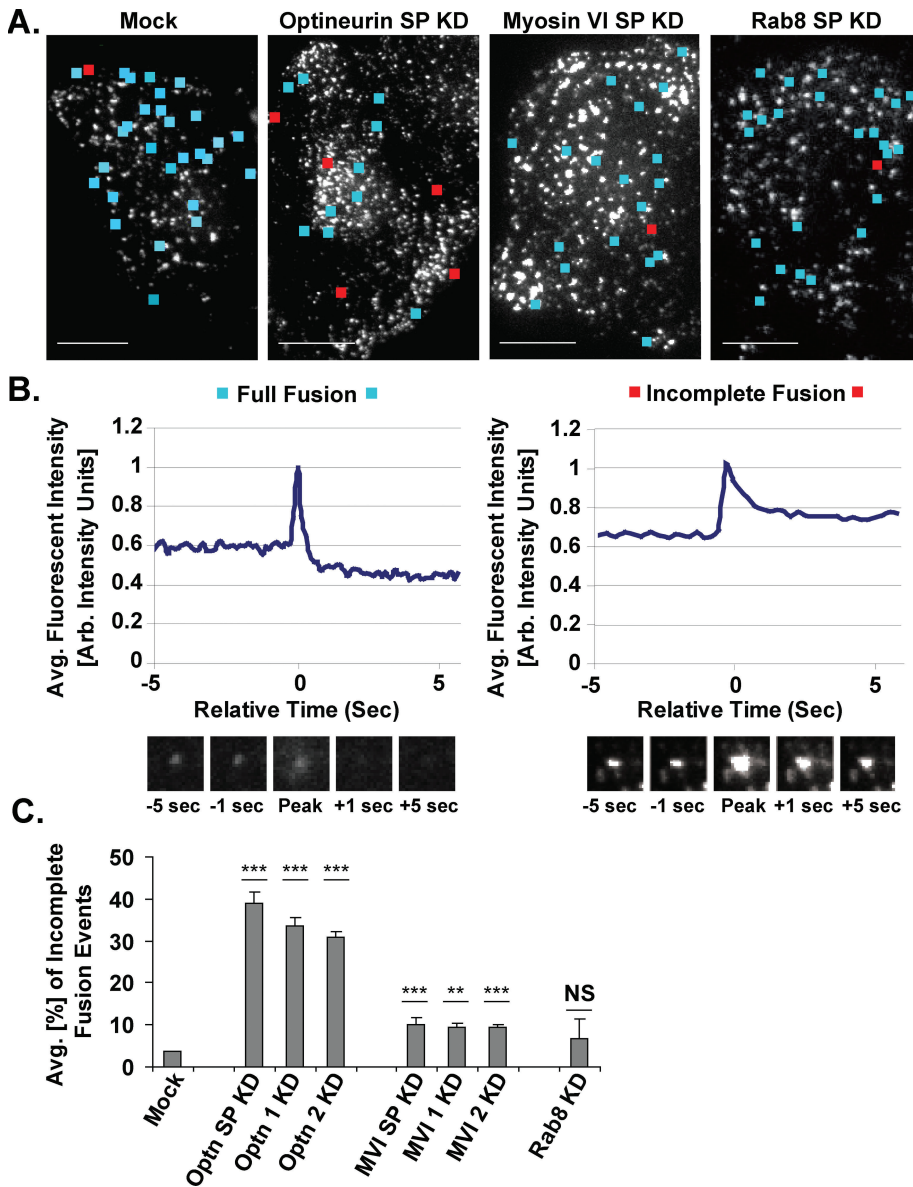


FIGURE 6: Full vs. incomplete fusion events at the plasma membrane. (A) Sample images of the TIRF field of mock and knockdown cells with locations of full fusion events during a 20-s movie marked with blue squares and the incomplete fusion events with red squares. Bar, 10 μ m. (B) Representative profiles of average intensity vs. relative time for localized regions containing full vs. incomplete fusion events. Before plotting, all intensities were corrected for photobleaching and normalized to a peak value of 1. The images display the fusing vesicle at the peak of the plot and at 1- and 5-s time points before and after this peak. (C) Average proportion of incomplete vesicle fusion events observed by TIRF microscopy at the base of sets of cells monitored at specific, 5-min intervals between 25 and 60 min after AP21998 addition. Knockdown of optineurin with SMARTpool primers (SP) results in a ninefold increase in the proportion of incomplete fusion events (unpaired t test; $n = 4$ sets of 10 cells; $p = 2 \times 10^{-5}$) and knockdown with individual primer 1 or individual primer 2 results in an eightfold increase (unpaired t test; $n = 4$ sets of five cells each; $p = 6 \times 10^{-6}$, $p = 1 \times 10^{-6}$). Knockdown of myosin VI with SMARTpool primers (SP), individual primer 1, or individual primer 2 results in 1.7-, 1.6-, and 1.7-fold increases in the percentage of incomplete vesicle fusion events, respectively (unpaired t test; $n = 5$ sets of 10 cells each [SP] or 4 sets of five cells each [individual primers]; $p = 1 \times 10^{-4}$, $p = 0.003$, $p = 3 \times 10^{-5}$). Knockdown of Rab8 has no significant effect on the proportion of incomplete fusion events (unpaired t test; $n = 3$ sets of 10 cells; $p = 0.4$). Bar, SEM. * $p \leq 0.05$, ** $p \leq 0.01$, *** $p \leq 0.001$.

itself been separately implicated in the regulation of fusion pore expansion and contraction (Larina *et al.*, 2007; Cingolani and Goda, 2008). Specifically, it has been suggested that myosin II and cortical

actin together promote the increased membrane tension necessary to expand the fusion pore for full content release (Berberian *et al.*, 2009). Membrane remodeling through the interaction of myosin Ic and the actin cytoskeleton has been similarly shown to play a role in exocytic vesicle fusion in mouse adipocytes (Bose *et al.*, 2004) and in compensatory endocytic vesicle formation in *Xenopus laevis* (Sokac *et al.*, 2006).

Though initiation of fusion at the plasma membrane is closely tied to the functioning of SNARE proteins, Sec1/Munc18 homologues (SM proteins), and Rab proteins (Jahn and Sudhof, 1999; Stenmark, 2009; Jackson, 2010; Pieren *et al.*, 2010), the specific molecular mechanism regulating fusion pore expansion and closure remains to be determined. Several factors other than myosin II/myosin Ic and actin have also been implicated in the regulation of fusion pore mechanics, such as calcium concentration (Elhamdani *et al.*, 2006), cholesterol levels (Wang *et al.*, 2010), the SNARE-binding proteins complexin II (Archer *et al.*, 2002) and synaptotagmin (Davis *et al.*, 1999; Rizo *et al.*, 2006), and the GTPase dynamin (Tsuboi *et al.*, 2002; Jaiswal *et al.*, 2009), but the interaction between these factors on a mechanistic level is presently unclear. Our study adds to the list of likely players in this process both optineurin and myosin VI.

The similar functional defects in secretion after myosin VI or optineurin knockdown (reduced secretion levels, increased proportion of docked vesicles at the plasma membrane, and increased number of incomplete fusion events) suggest a coordinated function for these proteins at the fusion pore. As such, we propose a model whereby the optineurin and myosin VI present on secretory vesicles at the plasma membrane function together in fusion pore regulation (Figure 7). Given the high level of colocalization between myosin VI and secretory vesicles in the TIRF field, we suggest that myosin VI is recruited to docked secretory vesicles, perhaps by binding to PtdIns(4,5)P₂, a phospholipid known to function both in exocytosis (Wenk and De Camilli, 2004) and in the recruitment of myosin VI to clathrin-coated endocytic vesicles (Spudich *et al.*, 2007). On the basis of the low-level colocalization of optineurin with secretory vesicles in the TIRF field, we suggest that optineurin is recruited to vesicles immediately prior to fusion (possibly by the already present myosin VI) and binds to a yet-to-be-determined member of the fusion pore machinery. The functional connection between huntingtin, a known binding partner of optineurin, and complexin II suggests huntingtin as one possible link between optineurin and the fusion

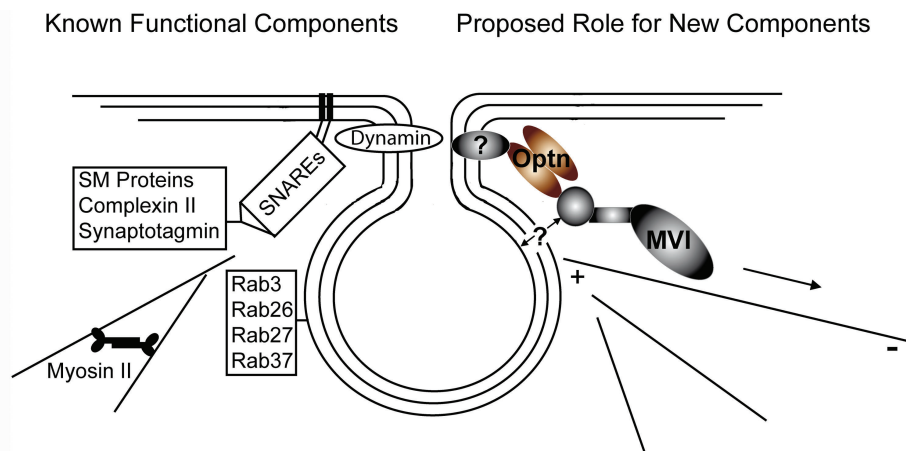


FIGURE 7: Suggested model for involvement of optineurin and myosin VI in fusion pore expansion. Fusion pore formation and regulation are presently tied to certain SNARE proteins and Rab GTPases, Sec1/Munc18 homologues (SM proteins), the SNARE-binding proteins complexin II and synaptotagmin, the GTPase dynamin, and the molecular motors myosin II and myosin 1c. Our data suggest that the myosin VI and optineurin present on secretory vesicles at the plasma membrane also function at the fusion pore. We propose that optineurin binds an unidentified protein associated with the fusion pore, in addition to the myosin VI previously recruited to docked secretory vesicles. In this manner, a functional link is formed between the fusion pore and the actin cytoskeleton associated with myosin VI. This link permits the use of the tensile forces created by movement of myosin VI toward the inward-facing minus ends of actin filaments to stabilize or expand the fusion pore. In short, we propose that optineurin and myosin VI regulate fusion pore dynamics by acting as a link between the fusion pore and the tensile forces of the actin cytoskeleton.

pore machinery (Edwardson *et al.*, 2003). In light of our functional TIRF studies, we suggest that the fusion pore-bound optineurin functions with the myosin VI previously recruited to docked secretory vesicles to anchor the fusion pore to the actin cytoskeleton. The movement of optineurin-bound myosin VI toward the inward-directed minus ends of actin filaments at the plasma membrane would thereby provide the tension necessary for stabilization and expansion of the fusion pore. Overall, we propose a model in which optineurin and myosin VI serve as one interface between the fusion pore regulatory machinery and the tension-providing modulations of the actin cytoskeleton.

It is important to note that this model provides only one possibility for the function of myosin VI and optineurin in fusion pore formation. Given that myosin VI and optineurin colocalize with cargo-filled vesicles at very different levels and that myosin VI and optineurin knockdown cells show proportionally different increases in incomplete fusion events, it is also possible that these proteins function separately in the mechanism of fusion pore expansion and closure. Such independent functionality would explain the lack of effect of a Rab8 knockdown on the number and type of secretory fusion events at the plasma membrane, which suggests that the Rab8–optineurin–myosin VI complex shown to be required for cargo sorting in polarized epithelial cells (Au *et al.*, 2007) does not function in fusion pore expansion.

The biomedical implications of the involvement of myosin VI and optineurin in fusion pore dynamics are very interesting; recent work points to the emerging fusion pore regulation machinery as a critical control point for the regulation of release of the contents of secretory vesicles (Thorn, 2009). It is possible, therefore, that the malignant progression of diseases aggravated by mutations in optineurin or myosin VI may stem from improper regulation of levels of secretory cargo release. For example, secretory defects in myocilin and angiotensin-like 7 protein secretion have been linked to the pro-

gression of POAG, a disease often caused by mutations in optineurin (Joe *et al.*, 2003; Kuchtey *et al.*, 2008). Patients with ALS, a disease causally linked to improper optineurin function, also demonstrate abnormal secretion of growth hormone and insulin-like growth factor (Maruyama *et al.*, 2010; Pellicchia *et al.*, 2010). Alteration in secretion levels of brain natriuretic peptide has been shown to mark disease progression in hypertrophic cardiomyopathy, a disease linked to mutations in myosin VI (Pieroni *et al.*, 2007). Furthermore, it has been suggested that the overexpression of myosin VI in prostate cancer cells enhances disease progression by increasing secretion of proteins such as vascular endothelial growth factor (Puri *et al.*, 2009). Our study of the effects of myosin VI and optineurin on secretion level modulation via fusion pore dynamics is therefore a new avenue for understanding the involvement of these proteins in disease malignancy.

MATERIALS AND METHODS

Antibodies

The following antibodies were used: rabbit polyclonal antibody to optineurin (Sahlender *et al.*, 2005); rabbit polyclonal antibody to myosin VI (Buss *et al.*, 1998), mouse monoclonal antibody to Rab8 (BD Transduction Laboratories, Franklin Lakes, NJ), mouse monoclonal antibody to VAMP7 (Gordon *et al.*, 2010), mouse monoclonal antibody to syntaxin5 (Williams *et al.*, 2004), rabbit polyclonal antibody to Dab2 (Santa Cruz Biotechnology, Heidelberg, Germany), rabbit polyclonal antibody to calregulin (Santa Cruz Biotechnology), rabbit polyclonal antibody to DsRed (Clontech, Mountain View, CA), and mouse monoclonal antibody to GFP (Invitrogen, Paisley, UK).

Cell lines and expression constructs

The reporter construct secretion system was developed by Andrew Peden from the RPD Regulated Secretion/Aggregation Kit (Ariad Pharmaceuticals) as previously described (Gordon *et al.*, 2010). In short, eGFP (Clontech) was incorporated into the pC4S1-FM4-FCS-hGH plasmid from this kit. The section of this plasmid containing the eGFP, signal sequence, aggregation domains, furin cleavage site, and human growth hormone was then transferred into a retroviral vector (pQCXIP; Clontech). The resulting pQCXIP-S1-eGFP-FM4-FCS-hGH construct was used to generate a stable secretion cell line in HeLa-M cells. To initiate secretion during microscopy studies, cells were treated with a 1- μ M solution of AP21998, a ligand which solubilizes the reporter molecule by interrupting the interaction of its aggregation domains.

The GalT-mRFP plasmid used in this work was provided by G. Patterson (Lippincott-Schwartz Lab, National Institute of Child Health and Human Development, Bethesda, MD).

Cell culture and transfection

The cell line used in this study was maintained at 37°C in Dulbecco's modified Eagle medium (Invitrogen) supplemented with 10% fetal calf serum (FCS), 2-mM L-glutamine, and penicillin/streptomycin (Sigma-Aldrich, Dorset, UK). To maintain selection

for cells containing the pQCXIP-S1-eGFP-FM4-FCS-hGH construct, this medium was also supplemented with puromycin (1.66 µg/ml).

Transfection of the GalT-mRFP or myosin VI-mCherry plasmids into tissue culture cells was executed according to the instructions provided by the manufacturer of the FuGENE transfection reagent (Roche Diagnostics, Welwyn Garden City, UK). Prior to transfection, cells were grown to 50% confluence on a six-well tissue culture tray (Greiner Bio-One, Stonehouse, UK). Two micrograms of plasmid DNA and 6 µl of FuGENE transfection reagent diluted in 95 µl of Optimem I medium (Invitrogen) were used for each given transfection in one well of the six-well tray.

Immunofluorescence

For immunofluorescence experiments, cells transfected 24 h prior with the appropriate constructs were treated with AP21998 for 35 min, fixed with 4% paraformaldehyde in phosphate-buffered saline (PBS) for 20 min, permeabilized in 0.2% Triton X-100 in PBS for 5 min, and blocked in 1% bovine serum albumin in PBS for 30 min. After blocking, cells were incubated with primary antibodies (polyclonal antibody to DsRed (Clontech) or polyclonal antibody to optineurin; monoclonal antibody to GFP [Invitrogen]) and then with secondary antibodies (goat anti-rabbit IgG coupled with Alexa 555; goat anti-mouse IgG coupled with Alexa 488 [Invitrogen]). After washing, cells were mounted on glass slides with Prolong Gold Antifade Mounting Reagent (Molecular Probes, Invitrogen, United Kingdom) and imaged on a Zeiss TIRF 3 microscope (Carl Zeiss, Welwyn Garden City, UK).

RNAi experiments

ON-TARGET plus SMARTpool mixtures of four individual primers (Dharmacon, Cramlington, UK) were used for depletion of myosin VI, optineurin, and Rab8. Individual primers to myosin VI (MVI 1, 5'-CAUUGUAUCUGGAGAAUCAUU-3'; MVI 2, 5'-ACAUUCUGAUUGCAGUGAAUU-3') and optineurin (Optn 1, 5'-CUUCGAA-CAUGAGGAGUUA-3'; Optn 2, 5'-CUAUGGCCUUGAGUCAUG-3') were used to verify results and control for off-target effects.

For efficient siRNA knockdown of myosin VI, optineurin, or Rab8, we used a double-knockdown protocol in which cells were transfected with siRNA primers on days 1 and 3 using Oligofectamine (Invitrogen) according to the manufacturer's instructions. Before siRNA knockdown, cells were grown to 70% confluence in a six-well tray. For each knockdown, siRNA primers were diluted in Optimem I and transfected into individual wells of the six-well tray at a final concentration of 90 nM. The effectiveness of the knockdown was checked by immunoblotting on day 4 and efficiently depleted cells were imaged on day 5. A similar double-knockdown protocol was used for depletion of syntaxin5, but transfections were conducted with a single Dharmacon siRNA primer (5'-GGACAUCAAUAGCCUCAAC-3') at a 40-µM final concentration using Lipofectamine 2000 (Invitrogen).

VAMP7 was depleted in a single-hit siRNA transfection protocol with a single Dharmacon primer (5'-GAACCUCACAGCUCACUAUU-3') at a final concentration of 90 nM using Oligofectamine. The effectiveness of the knockdown was checked by immunoblotting on day 3 and efficiently depleted cells were imaged on day 4.

Mock-transfected cells were treated with the same mixture of Oligofectamine/Lipofectamine 2000 in Optimem I as siRNA-transfected cells, but the solution used for these mock cells contained no siRNA.

Immunoblotting

Immunoblotting was used to assess whether individual proteins had been efficiently depleted by our siRNA knockdown protocol. To

prepare protein samples for this process, mock and knockdown cells were resuspended in urea/β-mercaptoethanol loading buffer (2% SDS, 30% glycerol, 1 M β-mercaptoethanol, 6 M urea, 0.125 M Tris, pH 6.8, and 0.01% bromophenol blue), lysed, and then boiled for 4 min. SDS-PAGE of protein samples was carried out on 10 or 12% polyacrylamide gels as previously described (Matsudaira and Burgess, 1978). A Dual Color Precision Plus Protein Standard (Biorad, Bath, UK) was loaded at either end of the gel as a reference for comparison of molecular weights of protein samples. After electrophoresis, a semidry blotter was used to transfer proteins from the SDS-polyacrylamide gel to a Protran nitrocellulose membrane with a pore size of 0.45 µm (Schleicher and Schuell Bioscience, London, UK). The membrane was incubated in 10% wt/vol Marvel milk powder in 1× PBS to block nonspecific binding sites. Individual sections of membrane containing specific proteins of interest were then incubated with primary and then secondary antibodies diluted in 1% wt/vol Marvel milk powder in 1× PBS. An enhanced chemiluminescence reaction kit (GE Healthcare, Amersham, UK) was used to detect protein bands in the membrane.

Spinning disc microscopy

For spinning disc microscopy studies, cells were grown on 25-mm round coverslips (VWR International, Lutterworth, UK) and imaged at 37°C in CO₂-independent medium (Invitrogen). Images were obtained on a Zeiss Cell Observer SD microscope (Carl Zeiss) using a 63× or 100× lens and 2 × 2 binning. Images were acquired with a Hamamatsu Photonics EM-CCD Digital Camera (Hamamatsu City, Japan) and AxioVision imaging software (Carl Zeiss).

Volocity analysis software (Improvision, Cambridge, UK) was used to quantify the rate of transfer of the reporter molecule from the ER to the Golgi complex in spinning disc videos.

TIRF microscopy

For live-cell TIRF microscopy studies, cells were grown on 25-mm round coverslips (VWR International) and imaged at 37°C in CO₂-independent medium (Invitrogen). Imaging was conducted on a Zeiss TIRF 3 microscope (Carl Zeiss). During each TIRF experiment, a 488-nm argon laser was directed at the coverslip at an angle greater than the critical angle of the laser line. The resulting total internal reflection of the laser line created an evanescent field in the 100–200-nm region of the sample closest to the coverslip.

Images were acquired with a 100× lens, Hamamatsu Photonics EM-CCD digital camera (Hamamatsu Photonics), and AxioVision Imaging Software (Carl Zeiss). Samples were imaged in 5-min intervals at maximum speed (approximately 4 frames/s) at points 25, 32, 39, 46, and 53 min after the addition of 1 µM AP21998. Exactly two cells were imaged at each time point to ensure that the distribution of cells over the course of the imaging period was equivalent between mock and knockdown data sets.

The total area covered by docked vesicles at the base of a given cell was calculated from the first frame of each movie using Volocity Analysis software (Improvision). This software was also used to profile fluorescent intensity over time at the sites of individual full or incomplete fusion events.

Vesicle tracking program

The number of vesicles traveling in 6 µm × 6 µm regions between the *trans*-Golgi and the plasma membrane in spinning disc videos was quantified using a customized particle tracking program. This program was modified by C.A. Combs (Light Microscopy Core Facility at the National Heart, Lung, and Blood Institute) and R. Kling (Ronn Kling Consulting, Warrenton, VA) from open-source particle

tracking software developed by D. Grier (New York University), J. Crocker (University of Pennsylvania), and E.R. Weeks (Emory University). The customized program allows for image segmentation through a combination of manual and computer-aided image segmentation and particle identification in combination with quantification of movement rates. The program was developed and run through the programming software IDL (ITT Visual Information Solutions, Boulder, CO). During analysis, all vesicle tracks were manually screened for accuracy in resolving the distinct movements of individual vesicles prior to data analysis. Data collected for a given region were exported as a tab-delimited file to a version of Origin-Pro analysis software (OriginLab, Northampton, MA) formatted to interface with the tracking program.

Image processing

Individual images were processed in Adobe Photoshop, and figures were assembled in Adobe Illustrator.

ACKNOWLEDGMENTS

We thank G. Patterson (Lippincott-Schwartz Lab, National Institute of Child Health and Human Development) for the GalT-mRFP plasmid, M. Gratian and M. Bowen (Cambridge Institute for Medical Research [CIMR] Microscopy) for assistance with imaging and analysis, D. Gordon (Peden Lab, CIMR) for assistance with the assay cell line, and both C. Combs (National Institutes of Health [NIH] Light Microscopy Core Facility) and T. Sakamoto (Wayne State University) for assistance with the vesicle tracking software. This work was funded by the Wellcome Trust (F.B.), a scholarship from the Winston Churchill Foundation of the United States (L.B.), and an NIH-Oxford-Cambridge Ph.D. studentship (L.B.) and was supported by the Medical Research Council (J.K.-J.). The CIMR is in receipt of a strategic award from the Wellcome Trust.

REFERENCES

- Albillos A, Dernick G, Horstmann H, Almers W, Alvarez de Toledo G, Lindau M (1997). The exocytotic event in chromaffin cells revealed by patch amperometry. *Nature* 389, 509–512.
- Allan VJ, Thompson HM, McNiven MA (2002). Motoring around the Golgi. *Nat Cell Biol* 4, E236–E242.
- Archer DA, Graham ME, Burgoyne RD (2002). Complexin regulates the closure of the fusion pore during regulated vesicle exocytosis. *J Biol Chem* 277, 18249–18252.
- Au JS, Puri C, Ihrke G, Kendrick-Jones J, Buss F (2007). Myosin VI is required for sorting of AP-1B-dependent cargo to the basolateral domain in polarized MDCK cells. *J Cell Biol* 177, 103–114.
- Becker KA, Hart NH (1999). Reorganization of filamentous actin and myosin II in zebrafish eggs correlates temporally and spatially with cortical granule exocytosis. *J Cell Sci* 112 (Pt 1), 97–110.
- Berberian K, Torres AJ, Fang Q, Kisler K, Lindau M (2009). F-actin and myosin II accelerate catecholamine release from chromaffin granules. *J Neurosci* 29, 863–870.
- Bhat P, Thorn P (2009). Myosin 2 maintains an open exocytic fusion pore in secretory epithelial cells. *Mol Biol Cell* 20, 1795–1803.
- Bose A, Robida S, Furcinitti PS, Chawla A, Fogarty K, Corvera S, Czech MP (2004). Unconventional myosin Myo1c promotes membrane fusion in a regulated exocytic pathway. *Mol Cell Biol* 24, 5447–5458.
- Buss F, Kendrick-Jones J (2008). How are the cellular functions of myosin VI regulated within the cell? *Biochem Biophys Res Commun* 369, 165–175.
- Buss F, Kendrick-Jones J, Lionne C, Knight AE, Cote GP, Paul Luzio J (1998). The localization of myosin VI at the Golgi complex and leading edge of fibroblasts and its phosphorylation and recruitment into membrane ruffles of A431 cells after growth factor stimulation. *J Cell Biol* 143, 1535–1545.
- Caviston JP, Holzbaur EL (2009). Huntingtin as an essential integrator of intracellular vesicular trafficking. *Trends Cell Biol* 19, 147–155.
- Chibalina MV, Roberts RC, Arden SD, Kendrick-Jones J, Buss F (2008). Rab8-optineurin-myosin VI: analysis of interactions and functions in the secretory pathway. *Methods Enzymol* 438, 11–24.
- Chung le TK, Hosaka T, Harada N, Jambaldorj B, Fukunaga K, Nishiwaki Y, Teshigawara K, Sakai T, Nakaya Y, Funaki M (2010). Myosin IIA participates in docking of Glut4 storage vesicles with the plasma membrane in 3T3-L1 adipocytes. *Biochem Biophys Res Commun* 391, 995–999.
- Cingolani LA, Goda Y (2008). Actin in action: the interplay between the actin cytoskeleton and synaptic efficacy. *Nat Rev Neurosci* 9, 344–356.
- Davis AF, Bai J, Fasshauer D, Wolowick MJ, Lewis JL, Chapman ER (1999). Kinetics of synaptotagmin responses to Ca²⁺ and assembly with the core SNARE complex onto membranes. *Neuron* 24, 363–376.
- Disanza A, Scita G (2008). Cytoskeletal regulation: coordinating actin and microtubule dynamics in membrane trafficking. *Curr Biol* 18, R873–875.
- Donaldson JG, Lippincott-Schwartz J (2000). Sorting and signaling at the Golgi complex. *Cell* 101, 693–696.
- Doreian BW, Fulop TG, Smith CB (2008). Myosin II activation and actin reorganization regulate the mode of quantal exocytosis in mouse adrenal chromaffin cells. *J Neurosci* 28, 4470–4478.
- Edwardson JM, Wang CT, Gong B, Wytenbach A, Bai J, Jackson MB, Chapman ER, Morton AJ (2003). Expression of mutant huntingtin blocks exocytosis in PC12 cells by depletion of complexin II. *J Biol Chem* 278, 30849–30853.
- Egea G, Lazaro-Dieguez F, Vilella M (2006). Actin dynamics at the Golgi complex in mammalian cells. *Curr Opin Cell Biol* 18, 168–178.
- Elhamedani A, Azizi F, Artalejo CR (2006). Double patch clamp reveals that transient fusion (kiss-and-run) is a major mechanism of secretion in calf adrenal chromaffin cells: high calcium shifts the mechanism from kiss-and-run to complete fusion. *J Neurosci* 26, 3030–3036.
- Gordon DE, Bond LM, Sahlender DA, Peden AA (2010). A targeted siRNA screen to identify SNAREs required for constitutive secretion in mammalian cells. *Traffic* 11, 1191–1204.
- Griffiths G, Simons K (1986). The trans Golgi network: sorting at the exit site of the Golgi complex. *Science* 234, 438–443.
- Hattula K, Peranen J (2000). FIP-2, a coiled-coil protein, links Huntingtin to Rab8 and modulates cellular morphogenesis. *Curr Biol* 10, 1603–1606.
- Huber LA, de Hoop MJ, Dupree P, Zerial M, Simons K, Dotti C (1993a). Protein transport to the dendritic plasma membrane of cultured neurons is regulated by Rab8p. *J Cell Biol* 123, 47–55.
- Huber LA, Pimplikar S, Parton RG, Virta H, Zerial M, Simons K (1993b). Rab8, a small GTPase involved in vesicular traffic between the TGN and the basolateral plasma membrane. *J Cell Biol* 123, 35–45.
- Jackson MB (2010). SNARE complex zipping as a driving force in the dilation of proteinaceous fusion pores. *J Membr Biol* 235, 89–100.
- Jackson MB, Chapman ER (2006). Fusion pores and fusion machines in Ca²⁺-triggered exocytosis. *Annu Rev Biophys Biomol Struct* 35, 135–160.
- Jahn R, Sudhof TC (1999). Membrane fusion and exocytosis. *Annu Rev Biochem* 68, 863–911.
- Jaiswal JK, Rivera VM, Simon SM (2009). Exocytosis of post-Golgi vesicles is regulated by components of the endocytic machinery. *Cell* 137, 1308–1319.
- Joe MK, Sohn S, Hur W, Moon Y, Choi YR, Kee C (2003). Accumulation of mutant myocilins in ER leads to ER stress and potential cytotoxicity in human trabecular meshwork cells. *Biochem Biophys Res Commun* 312, 592–600.
- Keller P, Simons K (1997). Post-Golgi biosynthetic trafficking. *J Cell Sci* 110 (Pt 24), 3001–3009.
- Kuchtey J, Kallberg ME, Gelatt KN, Rinkoski T, Komaromy AM, Kuchtey RW (2008). Angiopoietin-like 7 secretion is induced by glaucoma stimuli and its concentration is elevated in glaucomatous aqueous humor. *Invest Ophthalmol Vis Sci* 49, 3438–3448.
- Larina O, Bhat P, Pickett JA, Launikonis BS, Shah A, Kruger WA, Edwardson JM, Thorn P (2007). Dynamic regulation of the large exocytotic fusion pore in pancreatic acinar cells. *Mol Biol Cell* 18, 3502–3511.
- Lee MC, Miller EA, Goldberg J, Orci L, Schekman R (2004). Bi-directional protein transport between the ER and Golgi. *Annu Rev Cell Dev Biol* 20, 87–123.
- Maruyama H et al. (2010). Mutations of optineurin in amyotrophic lateral sclerosis. *Nature* 465, 223–226.
- Matsudaira PT, Burgess DR (1978). SDS microslab linear gradient polyacrylamide gel electrophoresis. *Anal Biochem* 87, 386–396.
- Neco P, Fernandez-Peruchena C, Navas S, Gutierrez LM, de Toledo GA, Ales E (2008). Myosin II contributes to fusion pore expansion during exocytosis. *J Biol Chem* 283, 10949–10957.

- Noguchi T, Lenartowska M, Miller KG (2006). Myosin VI stabilizes an actin network during *Drosophila* spermatid individualization. *Mol Biol Cell* 17, 2559–2571.
- Palmer KJ, Watson P, Stephens DJ (2005). The role of microtubules in transport between the endoplasmic reticulum and Golgi apparatus in mammalian cells. *Biochem Soc Symp* 1–13.
- Pellecchia MT et al. (2010). The GH-IGF system in amyotrophic lateral sclerosis: correlations between pituitary GH secretion capacity, insulin-like growth factors and clinical features. *Eur J Neurol* 17, 666–671.
- Pieren M, Schmidt A, Mayer A (2010). The SM protein Vps33 and the t-SNARE H(abc) domain promote fusion pore opening. *Nat Struct Mol Biol* 17, 710–717.
- Pieroni M, Bellocchi F, Sanna T, Verardo R, Ierardi C, Maseri A, Frustaci A, Crea F (2007). Increased brain natriuretic peptide secretion is a marker of disease progression in nonobstructive hypertrophic cardiomyopathy. *J Card Fail* 13, 380–388.
- Presley JF, Cole NB, Schroer TA, Hirschberg K, Zaal KJ, Lippincott-Schwartz J (1997). ER-to-Golgi transport visualized in living cells. *Nature* 389, 81–85.
- Puri C, Chibalina MV, Arden SD, Kruppa AJ, Kendrick-Jones J, Buss F (2009). Overexpression of myosin VI in prostate cancer cells enhances PSA and VEGF secretion but has no effect on endocytosis. *Oncogene* 29, 188–200.
- Rezaie T et al. (2002). Adult-onset primary open-angle glaucoma caused by mutations in optineurin. *Science* 295, 1077–1079.
- Rizo J, Chen X, Arac D (2006). Unraveling the mechanisms of synaptotagmin and SNARE function in neurotransmitter release. *Trends Cell Biol* 16, 339–350.
- Rudolf R, Salm T, Rustom A, Gerdes HH (2001). Dynamics of immature secretory granules: role of cytoskeletal elements during transport, cortical restriction, and F-actin-dependent tethering. *Mol Biol Cell* 12, 1353–1365.
- Sahlender DA, Roberts RC, Arden SD, Spudich G, Taylor MJ, Luzio JP, Kendrick-Jones J, Buss F (2005). Optineurin links myosin VI to the Golgi complex and is involved in Golgi organization and exocytosis. *J Cell Biol* 169, 285–295.
- Saraste J, Svensson K (1991). Distribution of the intermediate elements operating in ER to Golgi transport. *J Cell Sci* 100 (Pt 3), 415–430.
- Sokac AM, Schietroma C, Gundersen CB, Bement WM (2006). Myosin-1c couples assembling actin to membranes to drive compensatory endocytosis. *Dev Cell* 11, 629–640.
- Sorensen JB (2009). Conflicting views on the membrane fusion machinery and the fusion pore. *Annu Rev Cell Dev Biol* 25, 513–537.
- Spruce AE, Breckenridge LJ, Lee AK, Almers W (1990). Properties of the fusion pore that forms during exocytosis of a mast cell secretory vesicle. *Neuron* 4, 643–654.
- Spudich G, Chibalina MV, Au JS, Arden SD, Buss F, Kendrick-Jones J (2007). Myosin VI targeting to clathrin-coated structures and dimerization is mediated by binding to Disabled-2 and PtdIns(4,5)P2. *Nat Cell Biol* 9, 176–183.
- Stenmark H (2009). Rab GTPases as coordinators of vesicle traffic. *Nat Rev Mol Cell Biol* 10, 513–525.
- Steyer JA, Almers W (2001). A real-time view of life within 100 nm of the plasma membrane. *Nat Rev Mol Cell Biol* 2, 268–275.
- Thorn P (2009). New insights into the control of secretion. *Commun Integr Biol* 2, 315–317.
- Tsuboi T, Terakawa S, Scalettar BA, Fantus C, Roder J, Jeromin A (2002). Sweeping model of dynamin activity. Visualization of coupling between exocytosis and endocytosis under an evanescent wave microscope with green fluorescent proteins. *J Biol Chem* 277, 15957–15961.
- Wang N, Kwan C, Gong X, de Chaves EP, Tse A, Tse FW (2010). Influence of cholesterol on catecholamine release from the fusion pore of large dense core chromaffin granules. *J Neurosci* 30, 3904–3911.
- Warner CL, Stewart A, Luzio JP, Steel KP, Libby RT, Kendrick-Jones J, Buss F (2003). Loss of myosin VI reduces secretion and the size of the Golgi in fibroblasts from Snell's waltzer mice. *EMBO J* 22, 569–579.
- Wells AL, Lin AW, Chen LQ, Safer D, Cain SM, Hasson T, Carragher BO, Milligan RA, Sweeney HL (1999). Myosin VI is an actin-based motor that moves backwards. *Nature* 401, 505–508.
- Wenk MR, De Camilli P (2004). Protein-lipid interactions and phosphoinositide metabolism in membrane traffic: insights from vesicle recycling in nerve terminals. *Proc Natl Acad Sci USA* 101, 8262–8269.
- Williams AL, Ehm S, Jacobson NC, Xu D, Hay JC (2004). rsl1 binding to syntaxin 5 is required for endoplasmic reticulum-to-Golgi transport but does not promote SNARE motif accessibility. *Mol Biol Cell* 15, 162–175.
- Zenisek D, Steyer JA, Almers W (2000). Transport, capture and exocytosis of single synaptic vesicles at active zones. *Nature* 406, 849–854.
- Zhou Z, Mislis S, Chow RH (1996). Rapid fluctuations in transmitter release from single vesicles in bovine adrenal chromaffin cells. *Biophys J* 70, 1543–1552.